# High Efficiency Drive of Dual Inverter Driven SPMSM with Parallel Split Stator

**Yongjae Lee* and Jung-Ik Ha***

**Abstract – This paper describes dual inverter drive for a fractional-slot concentrated winding permanent magnet synchronous machine (PMSM). PMSMs are widely used in many applications from small servo motors to few megawatts generators thanks to its high efficiency and torque density. Especially, fractional-slot concentrated winding PMSM is very popular in the applications where wide operation range is required because it shows very wide constant power speed ratios. High speed operation, however, requires lots of negative d-axis current for reducing back-EMF regardless of output torque. Field weakening current does not contribute to the torque generation in surface mounted PMSM case and causes inverter and copper loss. To reduce the losses from field weakening current, this paper proposes PMSM with split stator and parallel dual inverter drive. Proposed parallel dual inverter drive reduces back-EMF and enables efficient drive at high speed and light load situation. Control strategy of proposed dual inverter system is established through loss analysis and simulation. Proposed concept is verified with practical experiment.**

**Keywords: Dual inverter, Efficiency, Field weakening, High speed, Permanent magnet synchronous machine**

## 1. Introduction

Motor drive using permanent magnets has advantages of small size and high torque density. It also provides high efficiency because it needs no field current to make a rotor flux. Rotor flux from permanent magnet, however, generates high back-EMF at high speed region that restricts the operation range. So, permanent magnet synchronous machine (PMSM) system needs additional negative d-axis current to makes back-EMF low by inhibiting the flux linkage in high speed drive. Applications requiring field weakening operation are very wide from small servo motor drives to few hundred kilowatts machine drives including white appliances, industrial applications and electric vehicles (EVs). These applications require 2-15 times higher speed than the corner speed and field weakening control [1]-[3].

This field weakening characteristic of PMSM, however, not only constraints motor design but also causes lots of side effects. Most of all, efficiency at the field weakening range is relatively low comparing with below the corner speed because of additional copper loss and inverter loss caused by d-axis current. D-axis current also limits capability of output torque because it restricts q-axis current within limited rating current. In addition, field weakening drive requires look-up table about torque and speed or extra field weakening controller to decide amplitude of current. Look-up table based current reference generating method is widely used in industry and EV/HEV field because it takes account of the parameter variation, efficiency and individual characteristics of objective motor, although table for each machine is required. Field weakening controller based on output voltage feedback method is widely used for general purpose motor drive inverter because it is very convenient, reliable and parameter free. Additional field weakening controller, however, degrades dynamic performance of the machines at field weakening region [4]-[8].

This paper focused on the loss and efficiency of field weakening operation especially for light load case. D-axis current takes high proportion at light load because q-axis current is relatively small due to the light load requirement. Thus, d-axis current decides amplitude of phase current which causes inverter loss and copper loss of machine. In this case, efficiency of high speed range is dramatically dropped comparing with below the corner speed operation due to the additional copper loss and inverter loss caused by d-axis current.

In [9], dual inverter drive system configured as Fig. 1 is proposed for efficient high speed operation. The dual

* Dept. of Electrical and Computer Engineering, Seoul National University, Korea. (yongjaelee@snu.ac.kr, jungikha@snu.ac.kr)
Received 21 April 2013 ; Accepted 26 May 2013

inverter topology consists of parallel split two stators and two voltage source inverters (VSIs) which has common DC link. By using split stators, induced back-EMF to each inverter is reduced and it makes the d-axis current reduced. This paper is further research of the previous research [9].

This paper contains following subjects. Firstly, the topology of the dual inverter drive is introduced. And, the mathematical analysis of inverter loss and copper loss is accomplished. It includes the comparison of single inverter drive and dual inverter drive. Efficient drive strategy for proposed dual inverter system is also derived for various operating conditions. Finally, simulation and experimental results with the test motor are depicted and analyzed.

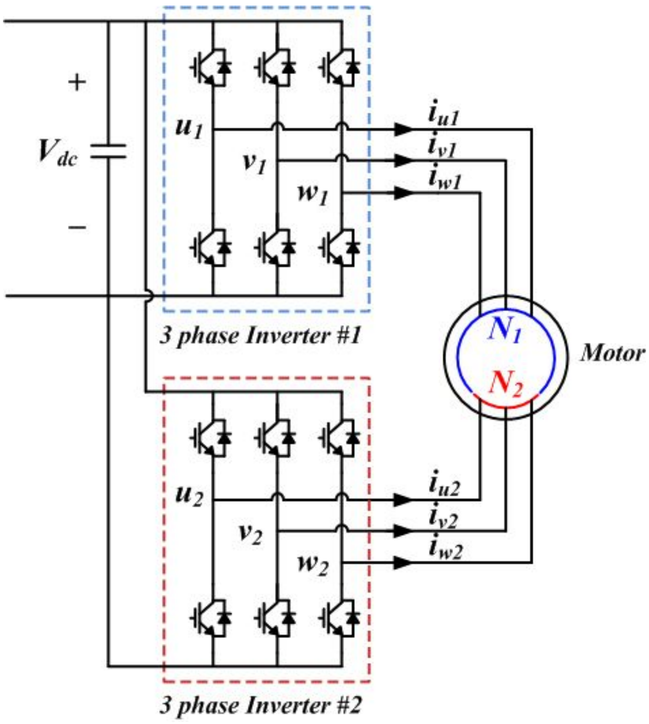


**Fig. 1.** Configuration of proposed dual inverter drive system

## 2. System Configuration

This section describes the structure of the proposed dual inverter drive system and analyzes the system and controller. This paper mainly considers fractional-slot concentrated-winding machine due to its very wide constant power speed ratio. This type of machines also have significantly high power density compared to the distributed winding machine. Fractional-slot concentrated-winding machine also has high efficiency at high load situation in low speed region. However, the efficiency sharply drops at high speed region due to the field weakening current. Thus, this paper especially focuses on the method to enhance the efficiency at light load high speed operation of fractional-slot concentrated-winding machine.

Fig. 2 shows the winding of fractional-slot concentrated-winding motor for parallel dual inverter drive. If the slots of the concentrated wound machine is divided as shown in Fig. 2, parameters of the machine such as inductance, $L_d$ and $L_q$, resistance, $R_s$, flux linkage made by permanent magnet, $\lambda_f$, will be divided with the stator split ratio, $D$, to each divided part in the ideal case when the side effects are neglected. With the specific description, $D$ can be defined with the number of slots for each part, $N_1$ and $N_2$, as

$$D = \frac{N_1}{N_1 + N_2}. \tag{1}$$

Then, the other parameters of the each divided part can be written as follows: $DL_d$, $DL_q$, $DR_s$ and $D\lambda_f$ for *Part #1* and $D'L_d$, $D'L_q$, $D'R_s$ and $D'\lambda_f$ for *Part #2* where $D'$ is $1\text{-}D$. In this paper, it is considered that *Inverter #1* feeds the *Part #1*, and *Inverter #2* feeds the residual *Part #2*. The control of dual inverter system is accomplished with similar method of parallel drive of individual two motors.

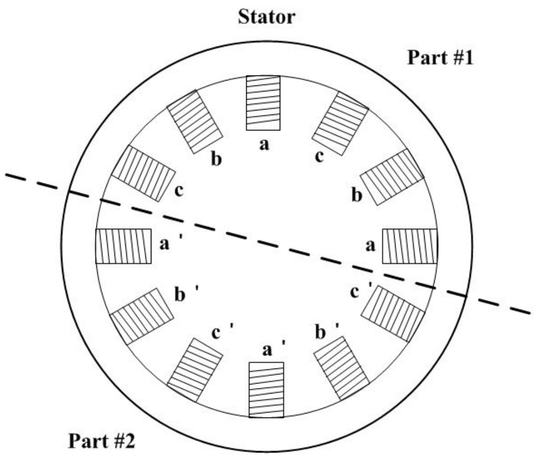


**Fig. 2.** Example of divided fractional-slot concentrated-winding machine

Reduced back-EMF constant, $D\lambda_f$ and $D'\lambda_f$, induces lower back-EMF voltage to both 3 phase inverters. Thus, the field weakening current for reducing back-EMF can be saved and used to generate output torque.

Proposed splitting stator winding method can be applied to not only the fractional-slot concentrated-winding machine but also distributed winding machine. To say the conclusion first, d-axis current decreases less for distributed winding case. Back-EMF decreases identically for both case because flux linkage reduces only according to the $D$. However, inductance of the distributed winding machine decreases proportional to $D^2$, not $D$. Thus, field weakening current have to be increased to reduce same amount of back-EMF for distributed winding case. For this reason, fractional-slot concentrated-winding machine has advantages to apply the proposed method.

Proposed parallel split motor is also proper for the applications where redundancy for safety is required. Because entire machine can be driven by only one inverter in accidental situation such as inverter breakdown, proposed method is more reliable than single inverter drive system. This characteristic is suitable for high safety integrity applications such as EV and electric railways. However in accident case, it cannot generate sufficient torque and efficiency also falls since the flux linkage is reduced and unpowered stator part where the broken inverter fed before generates core loss and magnet loss consistently due to the flux from permanent magnet.

Multi-phase inverter driven motor topology which studied before can be classified into two groups as shown in Fig. 3 [10]. Fig. 3(a) depicts the 6-phase motor drive system. This system consists of two 3-phase inverters which have 30° angle difference between both two inverters and windings. The 6-phase inverter has advantages in low torque ripple and the resultant voltage ripple of DC capacitor. However, 6-phase motor not only requires additional design factors such as slot/pole ratio but also has higher magnetic loss because magnetic flux is higher than that of the dual 3-phase drive system as shown in Fig. 3(b). The dual 3-phase inverter drive system has lower magnetic flux and suffers less from magnetic saturation problem. Proposed system also has design merit because it does not need a change from single inverter drive system. Of course it requires selection or split for optimal efficiency control.

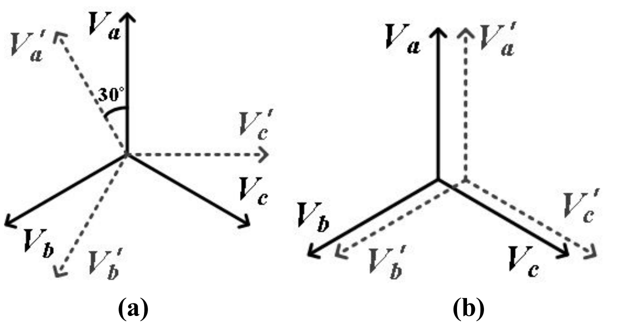


**Fig. 3.** (a) Vector diagram of 6-phase machine drive system (b) Vector diagram of proposed parallel split dual inverter drive system

Where the motor is divided equally, i.e. $D$=0.5, the electric characteristics are same for both split parts. It is also possible to drive the split motor with single inverter as shown in Fig. 4(b). If the system is constructed as in Fig. 4(b), only one inverter is necessary for the same operations of Fig. 4(a). However, this structure needs high current switching devices because of parallel driving. If parameters of two split parts are different with any reasons, large torque ripples are generated and efficiency will also drops. Because there are always parameter difference coming from mass production process, the independent feeding structure, Fig. 4(a), is recommended.

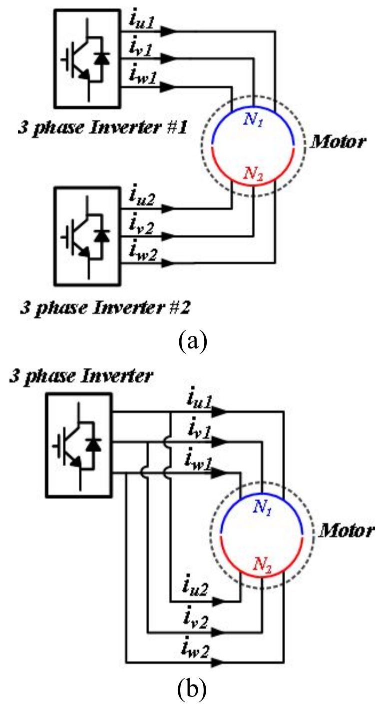


**Fig. 4.** (a) Individual feeding dual inverter system (b) Parallel drive of the single inverter system

Fig. 5 shows the block diagram of dual inverter system controller. Each inverter is controlled by independent current controller and each current controller is controlled by one common speed or torque controller. Torque divider generates each torque reference with output of the speed controller. The field weakening controller also works independently with current controller for other part.

This paper uses series split dual inverter drive system of Fig. 3(b) with independent two inverters depicted in Fig. 4(a). And fractional-slot concentrated-winding machine is used for better performance. Experiments and simulations are carried out in various speeds, torque dividing ratio with same stator split, and different stator split. Finally, analysis about efficiency and losses are accomplished.

## 3. Driving Strategy

This chapter describes the advantages of the proposed parallel drive in the perspective of efficiency and loss. The driving strategy considering the load and speed condition will be established also.

### 3.1 Loss Analysis

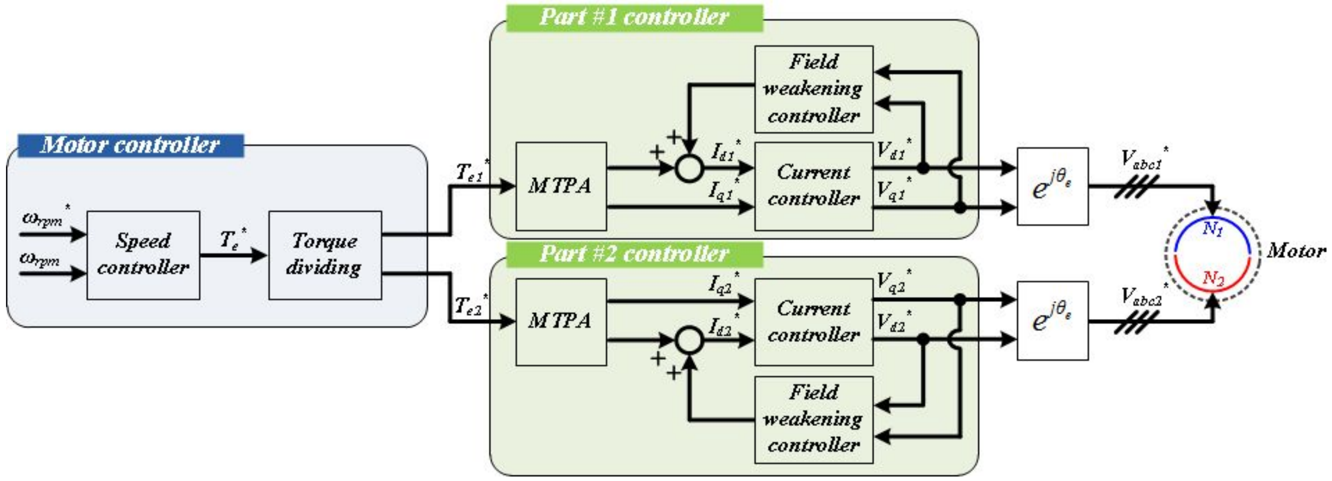


**Fig. 5.** Control block diagram of proposed parallel split dual inverter drive system

There are many sources of loss in the motor driving system. The losses in the motor drive system can be classified into three groups: inverter loss, machine loss and other driving system loss such as power consumption in controller, intelligent power module (IPM) and encoder, etc. Each loss is modeled and analyzed in many researches before. In this section, the representative models and analysis will be introduced.

Firstly, inverter loss will be analyzed. Inverter loss can be categorized again into two groups, conduction loss and switching loss. Conduction loss is generally modeled as a function of current and can simply modeled as

$$P_{con} = V_{CE} I , \tag{2}$$

where $P_{con}$ is the conduction loss, $V_{CE}$ is collector-emitter saturation voltage and $I$ is current flowing through the switch. Because $V_{CE}$ is generally proportional to the flowing current, conduction loss is proportional to square of the collector current.

Switching loss consists of turn-on loss, turn-off loss and reverse recovery loss of parasitic diode. These losses are hard to model and varying nonlinearly to the current and temperature. Thus, switching loss is generally approximated as a linear function of current and temperature. The coefficient of the approximated linear function can be achieved with datasheet of the selected switch. The further specific modeling and approximation are well introduced in [11].

Secondly, machine loss indicates the loss arose in machine itself and can be classified into copper loss and magnetic loss. Copper loss can be calculated easily as

$$P_{copper} = 1.5 I^2 R_s , \tag{3}$$

where $P_{copper}$ is copper loss in the machine and $R_s$ is lumped modeled stator resistance. Copper loss also varies according to the temperature and this effect has to be considered for precise estimation. Magnetic loss is hard to estimate and model since it contains lots of nonlinearity. Although magnetic loss estimation with finite elements method (FEM) is precise, it also contains non-ignorable errors. Thus, magnetic loss is commonly calculated with experimental parameters $k_e$ and $k_h$ [12]. And the equation is

$$P_{fe} = P_e + P_h = k_e \omega_e^2 \Phi^2 + k_h \Phi^\beta \omega_e , \tag{4}$$

where $P_{fe}$ is iron loss, $P_e$ is eddy-current loss, $P_h$ is hysteresis loss, $k_e$ and $k_h$ denotes the coefficients of the each loss, $\omega_e$ is electrical frequency of the flux, $\Phi$ is flux which flows through the core and β is steinmetz constant. Magnetic loss is not only hard to calculated exact value and also overlapped with other losses such as windage and stray loss.

Lastly, driving system loss indicates the loss due to the other driving system such as controller, IPM and encoder. The idle state loss becomes less than 1W in recent well designed machine driving system. However, once it starts to operate, the system loss increases due to the sensor, digital signal processing and gating circuit. And it is estimated approximately 5W. Thus, this value has to be considered in driving strategy.

### 3.2 Driving Strategy

As introduced in 3.1, loss caused in the system varies with operating condition. Thus, proper driving strategy has to be established to maximize the efficiency. Especially, since the proposed dual inverter system requires doubled system loss and reduces current at high speed region, further consideration about the operating strategy is essential.

As aforementioned in previous section, flux linkage is reduced in the proposed system according to the split ratio *D*. Thus, reduced output torque is generated with same amount of current for each inverter. However, the sum of the output torque from two parts has to be same with single inverter system. However, optimal current distribution for each inverter has to be considered for optimized control. Under heavy load case, high q-axis current is required and it causes high copper loss. Thus, only resistive model can be applied to the heavy load case. The objectives in high load case are satisfying output torque and minimizing loss. These objectives can be depicted as

$$T_e = T_1 + T_2 = \frac{3}{2}\frac{P}{2}(D\lambda_f I_{q1} + D'\lambda_f I_{q2}) \quad (5)$$

$$P_{loss} \cong \frac{3}{2}(DR_s I_{q1}^2 + D'R_s I_{q2}^2) \quad (6)$$

when only q-axis current is flowing, below corner speed. (5) shows the form of linear function and (6) shows the form of ellipse. The optimal current values can be found with mathematical and geometrical approach. Then, the solution of the problem is

$$I_{q1} = I_{q2}. \quad (7)$$

The result shows that currents have to be same for both inverters. And it can be interpreted that torque distribution between two stator parts has to be same with stator slot distribution ratio. Although the copper loss is minimized, inverter loss and system loss is increased when comparing with single inverter drive. Thus, efficiency of the proposed dual inverter drive at high load and low speed case is slightly lower than conventional method.

Under light load case, operation strategy have to be differed with speed region. Q-axis current is very small for both speed regions thanks to the partial load. D-axis current, however, is required for high speed operation not like low speed operation. Therefore, the amplitude of phase current is much higher for high speed drive case.

Below the corner speed region, copper loss and inverter loss is lower than system loss. By turning off one of two inverters, system loss can be minimized and inverter loss also can be mitigated. Although the loss from the turned-on inverter and stator part are increased due to the increased q-axis current, it is meaningful if the reduced system loss is higher than increased loss from turned-on inverter. The example of one inverter turned-off area can be drawn like Fig. 6. The break-even point, $T_{partial}$, varies with the system configuration and design. Thus, this break point should be decided with the experimental results of each applied system. This point goes upward for lossy system and goes downward for well-designed system.

Above the corner speed region, one inverter turned-off operation cannot be applied because power is regenerated through the parasitic diode of the turned-off inverter. Dual inverter driving, however, enables efficient driving because d-axis current is reduced at this region. This effect is much higher for the partial load case.

Voltage equations of PMSM in synchronous reference frame can be written as

$$V_d = R_d i_d - \omega_e L_q i_q + p(L_d i_d + \lambda_f), \quad (8)$$

$$V_q = R_q i_q + \omega_e (L_d i_d + \lambda_f) + p(L_q i_q). \quad (9)$$

where $V_d$ and $V_q$ are d and q axis voltages, $i_d$ and $i_q$ are d and q axis currents and $p$ is differential operator. The maximum synthesizable output voltage is limited and the area can be written with (8) and (9) as

$$(\omega_e L_d)^2 (i_d + \frac{\lambda_f}{L_d})^2 + (\omega_e L_q)^2 i_q^2 \le V_{\max}^2 \quad (10)$$

$$V_{\max} = \frac{V_{dc}}{\sqrt{3}}\eta \quad (11)$$

where $V_{max}$ is maximum synthesizable voltage, $V_{dc}$ is DC link voltage and $\eta$ is control margin, typically 0.9-0.95.

With the reduced parameters explained in previous section and (10), voltage limit ellipses of each inverter can be written as

$$(\omega_e L_d)^2 (i_{d1} + \frac{\lambda_f}{L_d})^2 + (\omega_e L_q)^2 i_{q1}^2 \le \left(\frac{V_{\max}}{D}\right)^2 \quad (12)$$

$$(\omega_e L_d)^2 (i_{d2} + \frac{\lambda_f}{L_d})^2 + (\omega_e L_q)^2 i_{q2}^2 \le \left(\frac{V_{\max}}{1-D}\right)^2. \quad (13)$$

It is clear that the radii of the ellipses written in (12), (13) is larger than that of single inverter case, (10), because $0 \leq D \leq 1$. Other characteristics is same for both systems except the radius. This effect can be interpreted as both increment of DC link voltage and decrement of effective speed. The difference of the voltage limit ellipses are described in Fig. 7. As shown in Fig. 7, voltage ellipse is larger with proposed parallel dual inverter drive system. Intersections of the current and voltage limit indicates the operable area of the system. Thus, proposed system, Fig.7(b), requires less d-axis current than single inverter system.

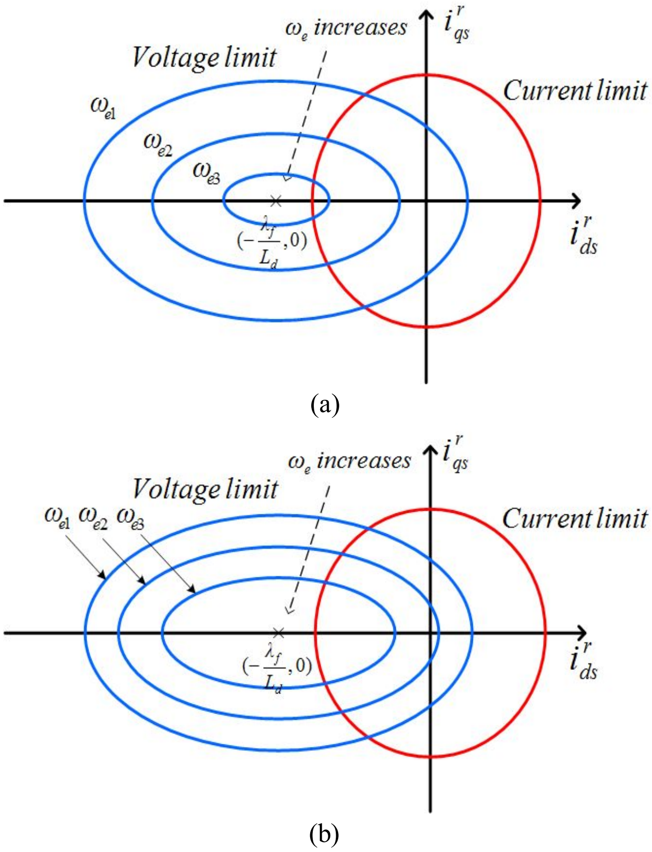


**Fig. 7.** Voltage and current limit of (a) single inverter drive system and (b) proposed dual inverter drive system ($\omega_{e1} < \omega_{e2} < \omega_{e3}$)

### 4. Simulation and Experimental Results

This paper has executed experiments with washing machine which rated power is 3kW to verify the validity of proposed dual inverter topology. Direct drive type washing machine motor needs not only wide operation area but also high output torque at low speed region. Thus the fractional-slot concentrated-winding machine is adequate machine for the purpose. Table 1. below shows the parameters of the machine used in the simulation and experiment.

**Table 1.** Parameters of the test motor

| ***Parameters*** | ***Value [unit]*** |
|---|---|
| $L_s$ ($L_d$, $L_q$) | 55 [*mH*] |
| $R_s$ | 6 [*Ω*] |
| $\lambda_f$ | 0.1735 [*V/(rad/s)*] |
| Slot/pole | 36/48 |
| Rated speed | 1200 [*r/min*] |
| Rated torque | 3 [*Nm*] |
| Maximum current | 3 [*A*] |

Switching device used in simulation and experiment is IGCM15F60GA made by Infineon, and used switching method is SVPWM with 16kHz switching frequency. All simulation and experiment use 85% of usable DC link voltage because of three-shunt current sensing [13]. DC voltage is regulated with 80% of 311V.

Switching and conduction characteristic varies non-linearly with current, voltage and temperature. Simulation assumes junction temperature of IGBT at 100°C and applies linear approximation for current and voltage. Fig. 8 to Fig. 10 are simulation results and Fig. 11 to Fig. 13 are experimental results with equally divided stator, *D=0.5*.

Fig. 8 shows the expected loss at rated speed and torque as a function of torque dividing ratio. Each graphs shows the aspect about different slot split ratio, $N_1$:$N_2$. As proved in previous section, loss is much smaller in dual inverter case. Equally divided stator case shows the lowest loss with equally divided torque. It shows that the loss is reduced about 60% of the single inverter drive case.

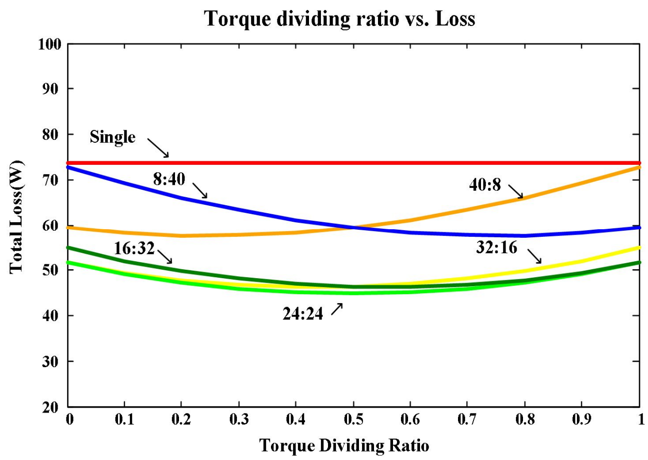


**Fig. 8.** Variation of total loss in proposed system as a function of torque dividing ratio with different stator dividing ratio

Fig. 9 shows the d-axis current of *Inverter #1* for entire operating range and for different slot split ratio, $N_1$:$N_2$. The absolute value of d-axis current is decreases with decreases of *D*. It also shows smaller d-axis current at above rated speed, i.e. it is possible to operate in higher speed with proposed method. Fig. 9 also shows no d-axis current in mid-speed range, 200-500rpm with proposed method when *D=0.5*.

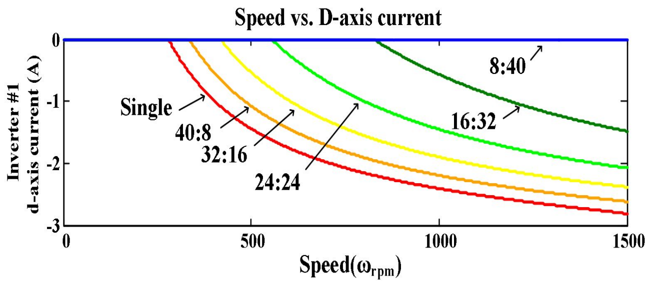


**Fig. 9.** Variation of d-axis current of proposed system as a function of speed with different stator dividing ratio

Fig. 10 shows the composition of loss where torque is optimally divided according to the variations of *D*. Loss mostly consists of copper loss and inverter loss and it does not change a lot with stator dividing ratio. However, copper loss changes significantly with changes of *D*, and it is reduced almost half of single inverter drive case when *D=0.5*. Fig. 10 also shows minimum loss appears when stator is equally divided as shown in Fig. 8.

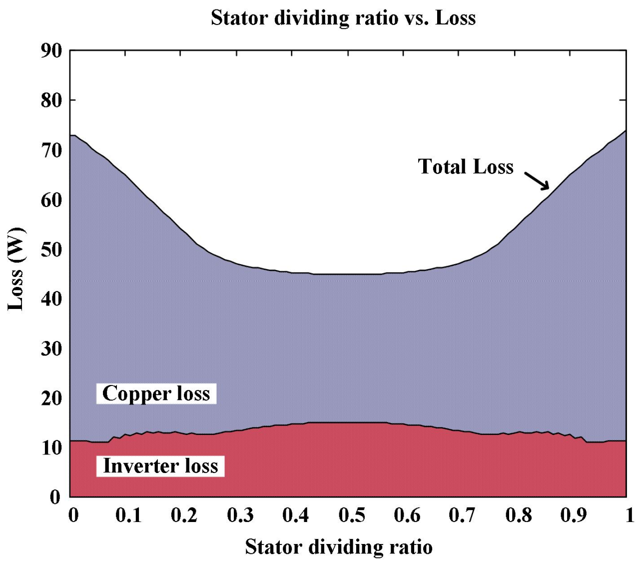


**Fig. 10.** Electrical loss composition of proposed dual inverter drive system.

Fig. 11 describes the input power to the system at rated torque and speed while varying the torque dividing ratio. Because it is hard to separates each loss component, input power to the system is compared. This figure also shows that 1:1 torque dividing is optimal choice when *D=0.5*. Experimental result shows almost 30W is saved at rated operating condition.

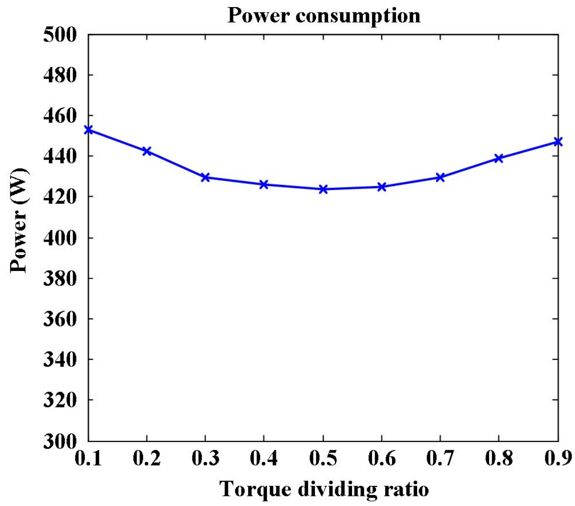


**Fig. 11.** Variation of power consumption in proposed system as a function of torque dividing ratio

Fig. 12 shows input power to the system at rated condition with different DC voltages and driving methods. In under fault situation, more q-axis current has to be flown to the normal part. And it generates lots of loss at machine and inverter. Core loss also exists at broken part due to the flux from permanent magnet. DC voltage variation also gives change of power dissipation. When DC voltage drops from 100% to 70% of normally distributed 220V AC source, power usage difference between single inverter drive and dual inverter drive increases because more d-axis current is required.

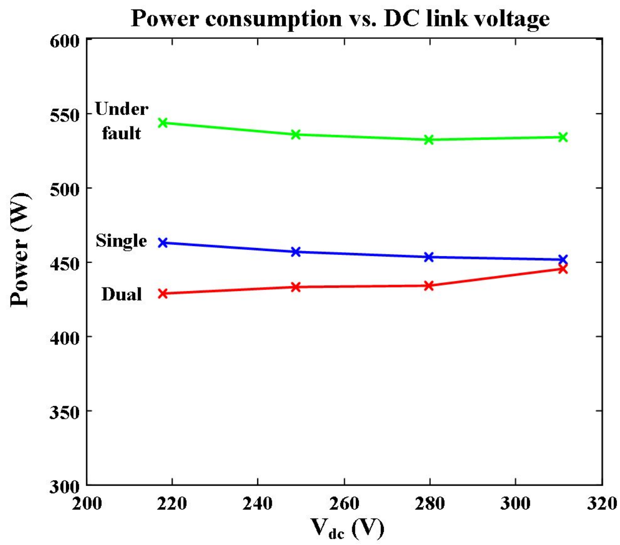


**Fig. 12.** Variation of power consumption in proposed system as a function of DC link voltage

It can be seen at Fig. 13 that the dual inverter drive uses more power at low speed region than single inverter drive system due to the increased inverter loss. As speed goes up, however, dual inverter drive system shows beneficial result than single inverter drive system because d-axis current is being injected. This power difference becomes wider with speed rising.

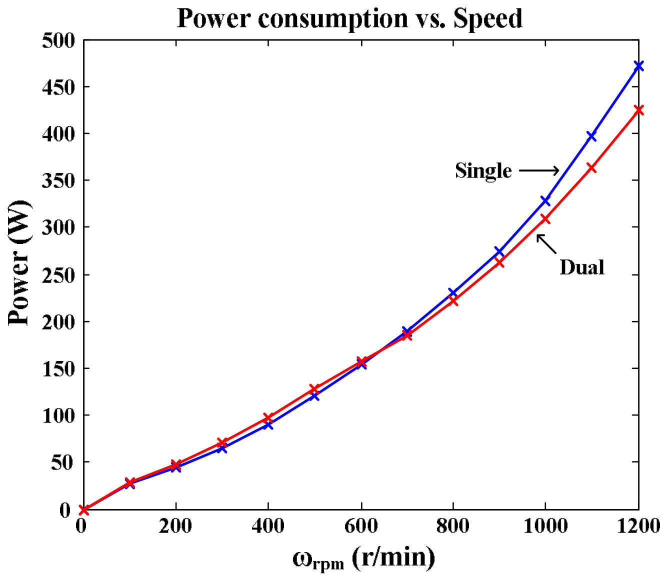


**Fig. 13.** Variation of power consumption as a function of speed for single and dual inverter system

## 5. Conclusion

As the environmental concerns are getting increased, it is more and more important for electric machine drive systems to minimize losses and enhance the efficiency. It is also true that the price of the power electronic device is getting down consistently. These trends motivate the researchers to study about machine drive system with many switches to increase the efficiency. This paper also proposes a kind of high efficiency drive system consists of two inverters. Split of the stator winding enables to reduce the back-EMF and mitigates d-axis current injection for field weakening. This paper analyzed the source of loss in the machine drive system and established the optimized drive strategy. With simulations and experiments, advantages of the proposed parallel dual inverter drive system are verified. Although the magnetic losses are neglected in the simulation and experiment, it is considered that the tendency is not different with the simulated results. Efforts to provide the analysis of magnetic loss through the FEM will be followed for further research.

## Acknowledgements

This research was supported by Basic Science Research Program through the National Research Foundation of Korea(NRF) funded by the Ministry of Science, ICT And Future Planning (2009-0083495)

## References

[1] K. C. Kim, "A novel magnetic flux weakening method of permanent magnet synchronous motor for electric vehicles," *IEEE Trans. Magn.*, vol.48, no. 11, pp. 4042-4045, Nov. 2012.
[2] R. Nalepa and T. Orlowska-Kowalska, "Optimum trajectory control of the current vector of a nonsalient-pole PMSM in the field-weakening region", *IEEE Trans. Ind. Electron.*, vol. 59, no. 7, pp. 2867-2876, Jul. 2012.
[3] D. Stojan, D. Drevensek, Z, Plantic, B. Grcar, and G. Stumberger, "Novel field-weakening control scheme for permanent-magnet synchronous machines based on voltage angle control," *IEEE Trans. Ind. Appl.*, vol.48, no. 6, pp. 2390-2401, Nov./Dec., 2012.
[4] C. Mademlis, I. Kioskeridis, N. Magaris, "Optimal efficiency control strategy for interior permanent-magnet synchronous motor drives," *IEEE Trans. Energy Convers.*, vol. 19, pp. 715-723, Dec. 2004.
[5] J. Lee, K. Nam, S. Choi, S. Kwon, "Loss-minimizing control of PMSM with the use of polynomial approximations," *IEEE Trans. Power Electron.*, vol. 24, pp. 1071-1082, Apr. 2009.
[6] T. Kwon, S. Sul, "Novel antiwindup of a current regulator of a surface-mounted permanent-magnet motor for flux-weakening control," *IEEE Trans. Ind. Appl.*, vol. 42, pp. 1293-1300, Oct. 2006.
[7] T. Kume, T. Iwakane, T. Sawa, T. Yoshida, I. Nagai, "A wide constant power range vector-controlled ac motor drive using winding changeover technique," *IEEE Trans. Ind. Appl.*, vol. 27, pp. 934-939, Sep./Oct. 1991.
[8] M. M. Swamy, T. Kume, A. Maemura, S. Morimoto, "Extended high-speed operation via electronic winding-change method for AC motors," *IEEE Trans. Ind. Appl.*, vol. 42, pp. 742-752, May/June, 2006.
[9] Y. Lee, J. Ha, "High efficiency dual inverter drives for a PMSM considering field weakening region," *Power Electronics and Motion Control Conference (IPEMC),* 2012, vol. 2, pp. 1009-1014.
[10] A. Tessarolo, C. Bassi, D. Giulivo, "Performance of a high-power induction motor supplied by two in-phase voltage source inverters," *in Proc. Int. Conf. Comp. as a Tool (EUROCON 2011)*, Apr. 2011, pp. 1-4.
[11] D. Chung, S. Sul, "Minimum-loss strategy for three-phase PWM rectifier," *IEEE Trans. Ind. Electron.*, vol. 46, no. 3, pp. 517-526, Jun. 1999.
[12] R. Dutta, M. Rahman, "Comparison of core loss prediction method for the interior permanent magnet machine," *in Proc. IEEE Int. Conf. Power Electron. Drives Syst.*, 2005, vol. 2, pp. 1396-1401.
[13] B. Cho, J. Ha, S. Sul, "Voltage injection method for boundary expansion of output voltages in three shunt sensing PWM inverters," *in Proc. 8th Int. Conf. Power Electron. (ICPE & ECCE)*, June 2011, pp.411-415.

**Yongjae Lee** received the B.S. and M.S. degrees in electrical engineering from Seoul National University, Seoul, Korea, in 2011 and 2013, respectively. He is presently pursuing the Ph.D. degree in Seoul National University. His research interests include electric machine drive for electric vehicles, renewable energy conversion.

**Jung-Ik Ha** was born in Korea in 1971. He received the B.S., M.S., and Ph.D. degrees in electrical engineering from Seoul National University, Seoul, Korea, in 1995, 1997, and 2001, respectively. From 2001 to 2002, he was a researcher in Yaskawa Electric Co., Japan. From 2003 to 2008, he worked for Samsung Electronics Co., Korea as a senior and principal Engineer. From 2009 to 2010, he was a chief technology officer, LS Mechapion Co., Korea. Since 2010, he has been an assistant professor of the School of Electrical Engineering, Seoul National University, Korea. His research interests are on circuits and control in high efficiency and integrated electric energy conversions for various industrial fields.